25
Fibre friction

25.1 Introduction

25.1.1 Historical development

The study of the friction of materials is based on the two classical 'laws' of friction, probably understood by Leonardo da Vinci, but rediscovered by Amontons in 1699. These laws state that the frictional force is independent of the area of contact between the two surfaces and is proportional to the normal force between them. They were verified by Coulomb in 1781. He also pointed out the distinction between static friction, the force that must be overcome in order to start sliding, and kinetic friction, the force resisting continued sliding. He observed that kinetic friction was independent of the speed of sliding; this is sometimes called the third law of friction. Mathematically, Amontons' law is expressed as:

$$F = \mu N \tag{25.1}$$

where F = frictional force acting parallel to the surface in a direction opposing relative movement. μ = coefficient of friction and N = force normal to the surfaces in contact.

When a yarn passes round a guide, as shown in Fig. 25.1, its tension must be increased by an amount necessary to overcome the frictional resistance. It follows from Amontons' law[1] that:

$$T_2 = T_1 \exp(\mu\theta) \tag{25.2}$$

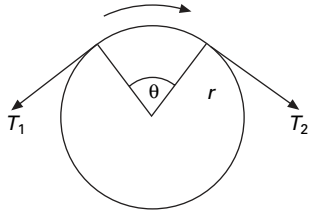

25.1 Values of $T_2/T_1 = e^{\mu\theta}$.

[1]Note devations from equation (25.2) due to bending, discussed in Section 25.2.2.

where T_2 = leaving tension, T_1 = incoming tension and θ = angle of contact.

In reality, these are not universal laws. The study of fibre friction has largely been the experimental observation of departures from the laws, the reasons for such departures, and their consequences. One of the earliest records is of the discovery by Monge in 1790 that the friction of wool depended on the direction in which the fibres were sliding.

25.1.2 Technological effects

The dualistic nature of the influence of friction on textile processing is illustrated by W. L. Balls's paradox: 'up to the front mule roller, cotton must be slippery; afterwards it must be sticky' [1]. Friction is the force that holds together the fibres in a spun yarn and the interlacing threads in a fabric. If the friction is too low, the yarn strength will fall, and the dimensional stability of cloth will be reduced. Here high friction is an advantage, enabling a greater proportion of the strength of the individual fibres to be utilised.

In many other places, however, fibre friction is a nuisance. If a yarn passes over a number of guides, the angle θ in equation (25.2) becomes the sum of the individual angles of contact. The figures in Table 25.1 show how rapidly the tension may increase in these circumstances. If excessive breaks are to be avoided, and the yarn is not to be permanently damaged by overstraining, it is essential to maintain the frictional resistance at as low a value as possible.

In the stitching of fabrics, high friction causes trouble for two reasons: the needle may become red-hot, and the threads will not slide over one another in order to allow the needle to pass between them. This causes many more threads to be broken; for example, in a particular unlubricated mineral khaki dyed cloth, there were nearly 20 cut threads per 100 needle punctures, but after lubrication the number of cut threads was insignificant [2].

Apart from these examples, where friction is clearly an advantage or a disadvantage, there are many other aspects of textile technology that are influenced by the frictional characteristics of the fibres: the handle and wear resistance of fabrics; the behaviour of fibres during drafting; and, especially in wool, the process of felting.

25.2 Measurement of fibre friction

25.2.1 Methods for fundamental studies

The apparatus developed by Bowden and Leben [3] is the best general method for the fundamental study of friction. Figure 25.2(a) illustrates its mode of operation. A

Table 25.1 Values of $T_2/T_1 = e^{\mu\theta}$

	$\theta = \pi/2$	$\theta = \pi$	$\theta = 2\pi$	$\theta = 4\pi$
$\mu = 0.2$	1.4	1.9	3.5	12.3
$\mu = 0.5$	2.2	6.0	22.9	525
$\mu = 1.0$	6.0	22.9	525	270 000

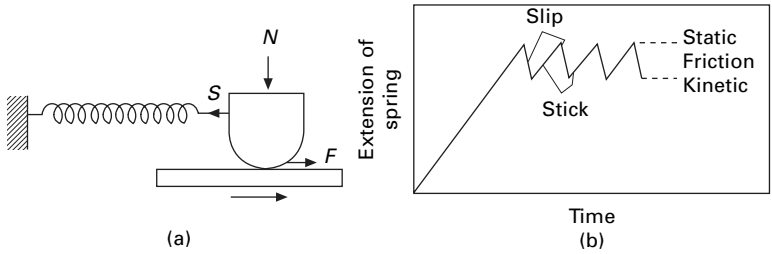

25.2 (a) Basic principle of Bowden and Leben's apparatus [3]. (b) Record of trace.

slider, under a load N, presses on a lower plate, which is moving past it at a constant velocity. The force of friction drags the slider along with the lower plate until the force S exerted by a spring fixed to the slider just balances the frictional force F. The extension of the spring is thus a measure of F. In practice, static friction F_s, the force opposing the start of slippage, is usually greater than kinetic friction F_k. Hence, once the slider has started to slip, it will be accelerated back until the tension in the spring has been reduced from a value equal to the force of static friction to that of the force of kinetic friction. The slider will continue to slip back for a further distance before it has decelerated and come to rest. It then moves forward again with the lower plate under the force of static friction. A record of the extension of the spring will give the 'stick–slip' trace shown in Fig. 25.2(b). If the damping is small, it can be shown that the force of kinetic friction is equal to the mean force exerted by the spring during the slip. Consequently, values of both F_s and F_k can be calculated when the characteristics of the spring are known.

In one practical form of this instrument [4, 5], suitable for loads between 5 mg and 100 g, the spring is a stiff wire beam, deflected horizontally by the movement of the slider, and deflected vertically to apply the load. The slider is carried on a turntable. For heavier loads [4, 5] of up to several kilograms, another form of the apparatus is used, with spring loading of the specimen and with the force opposing the drag of the specimen being applied by means of the rotation of a loaded bifilar suspension.

With these forms of apparatus, measurements of the friction of pads of fibres rubbing against solid surfaces may be made, and polymeric materials, of which fibres are made, may also be investigated, but for work on single fibres modifications are needed. The fibres may be mounted on frames under light tension and then pressed against one another, as is shown in Fig. 25.3. One fibre with its frame is then traversed along, and, in one form of the apparatus, the movement of the other is restrained by a leaf spring. The deflection of the spring may be recorded graphically with a stylus, or photographically by reflection from a mirror mounted on the spring, and gives a stick–slip trace from which the static and kinetic friction can be calculated. This method has been used by Mercer and Makinson [7]. In the similar instrument illustrated in Fig. 25.3 and used by Guthrie and Oliver [6], the 'stationary' fibre is suspended in a frame on a torsion wire, which rotates until the force is sufficient to cause slippage.

An ingenious development of this method for use with very light loads has been described by Pascoe and Tabor [8]. In their apparatus, shown in Fig. 25.4, the sliding

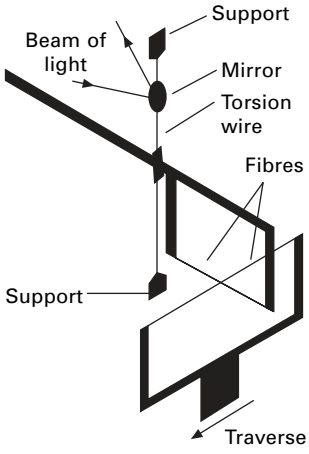

25.3 Essential features of Guthrie and Oliver's apparatus [6].

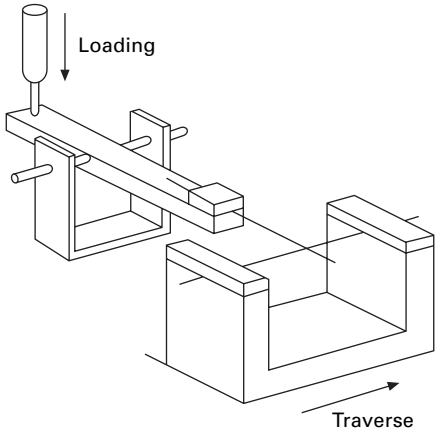

25.4 Measurement of fibre friction under very low loads [8].

fibre is mounted at one end only. The other end rests on the second fibre, which can be traversed along in a frame. The upper fibre acts as a cantilever. Its displacement in the vertical plane gives the load, and its displacement in the horizontal plane gives the force opposing the frictional drag. The displacements are determined by microscopical observation of the free end of the fibre.

The principles of these methods are still applicable for fundamental studies of fibre friction, but advances in transducers and detectors will lead to differences in detail.

25.2.2 Rapid methods

Whereas the above methods are the most suitable for fundamental investigations, they are less convenient for the rapid technical evaluation of frictional resistance. For

this purpose, there are advantages in the capstan method, which involves measurement of the excess tension needed to pull yarn over a guide. The basic feature of the apparatus is that shown in Fig. 25.1, and the coefficient of friction, assumed to be constant, can be calculated from the relation: $T_2/T_1 = \exp(\mu\theta)$. A static form of the method is illustrated in Fig. 25.5(a). A loop of fibre is placed over the guide and a small load placed on one side. The load on the other side is then decreased until slippage commences. Alternatively, a dynamic method may be used, with the yarn running continuously over the guide. Abbott and Grosberg [9] have described a version of the method suitable for use with an Instron Tensile Tester. Buckle and Pollitt [10] invented a mechanical tester in which the tensions operate in such a way that the coefficient of friction can be directly indicated by a pointer on a scale. However, this has been displaced by advances in electronic tension meters.

A typical modern instrument will have a means of pulling yarn over a guide, with tension meters on either side, as indicated schematically in Fig. 25.5(b). The springs are, in reality, stiff force transducers connected to a computer.

The simple derivation of equation (25.2) assumes that the yarn is perfectly flexible and does not take account of bending stiffness. As discussed in Section 19.5.4 in relation to flex fatigue testing, the form shown in Fig. 25.1 would have a discontinuity in bending moment at the point where it leaves the pin. In reality there will be a zone of changing curvature. An analysis by Jung *et al*. [11] also shows that the forces in the contact region are influenced by fibre stiffness. Equation (25.2) is a good approximation when the yarn or fibre radius is small compared with the pin radius, but Jung *et al*. [11] show that there are appreciable differences when a yarn passes over a guide at an angle. In a typical example, the value of T_2/T_1 increased by 20% in going from zero deviation to a 45° inclination. Another error in equation (25.2) results from bending hysteresis. Energy is dissipated not only in overcoming friction but also in the cycle of bending and unbending, which is undergone by each portion of material. The work done to provide this energy will appear to be a frictional loss and will cause the measured friction to be too large. Grosberg and Plate [12] have discussed the problem and shown that the error may be as high as 2.5%. The contribution

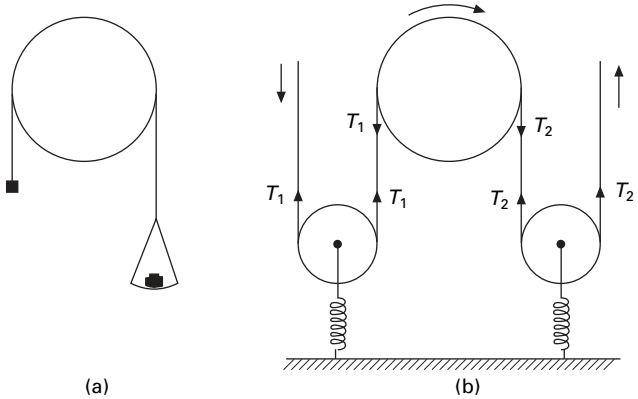

25.5 (a) Static capstan method. (b) Dynamic capstan method.

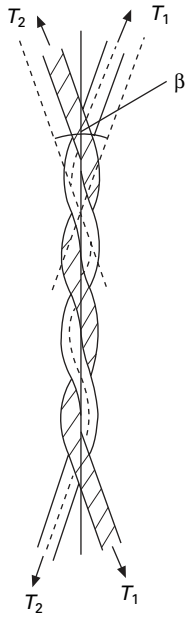

25.6 Measurement of inter-fibre friction [13].

to the frictional force is found to equal $\Delta M/r$, where ΔM is the difference in bending moment in bending and recovery and r is the radius of curvature of the capstan. The error may therefore be made negligible by using large cylinders.

For the measurement of inter-fibre friction, Lindberg and Gralén [13] introduced a method in which the two fibres are twisted together as shown in Fig. 25.6. If the difference between the tensions applied to the opposite ends of each fibre is increased, the fibres will eventually slip over one another. It is shown that:

$$\mu = \log_e \frac{T_2/T_1}{\pi n \beta} \tag{25.3}$$

where T_2 and T_1 are the tensions in the fibres, n is the number of turns of twist and β is the angle between the fibre axes and the axis of the twisted element.

The yarn-on-yarn abrasion tester shown in Fig. 25.7 can be adapted to measure friction in this way by adding tension meters or, as shown in Fig. 25.8, measurements can be made on a running yarn. Another variant of the method was used by Gupta and coworkers [14] to measure friction of sutures and hair [15]. This was adapted by Moghazy and Gupta [16] for testing in liquid.

Another technique that has been used to investigate fibre friction is the measurement of the force necessary to remove a single fibre from a mass of fibres under pressure [17], or to pull apart two interlocking fringes of fibres [18]. A convenient version of the latter method in which one fringe of fibres is pulled over another on an apparatus fitted to an Instron Tensile Tester is described by Hearle and Husain [19]. These measurements will be related to the practical behaviour of fibres in drafting and in yarns. Moghazy and Broughton [20] describe a method of using an Instron tester to pull a beard of cotton fibres from between metal plates.

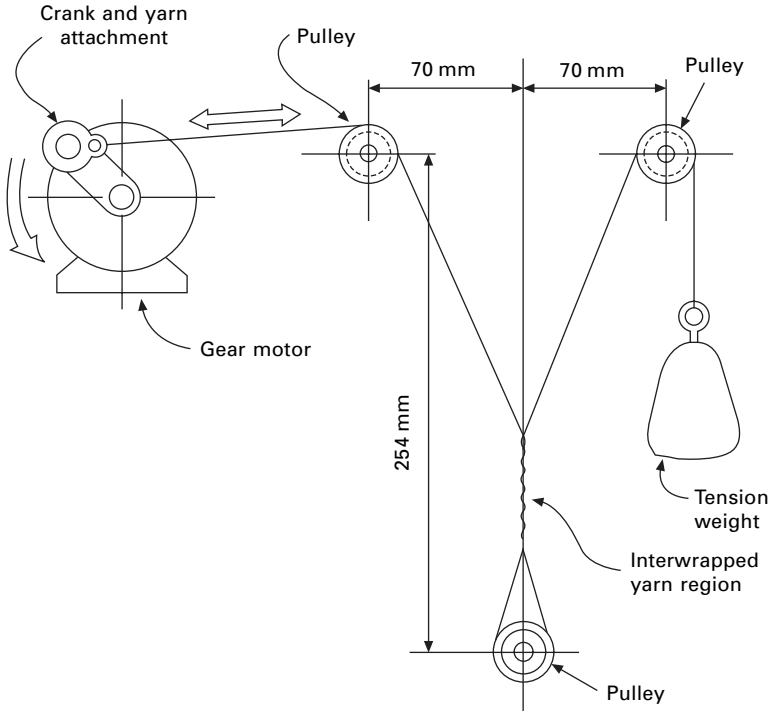

25.7 Yarn-on-yarn abrasion tester.

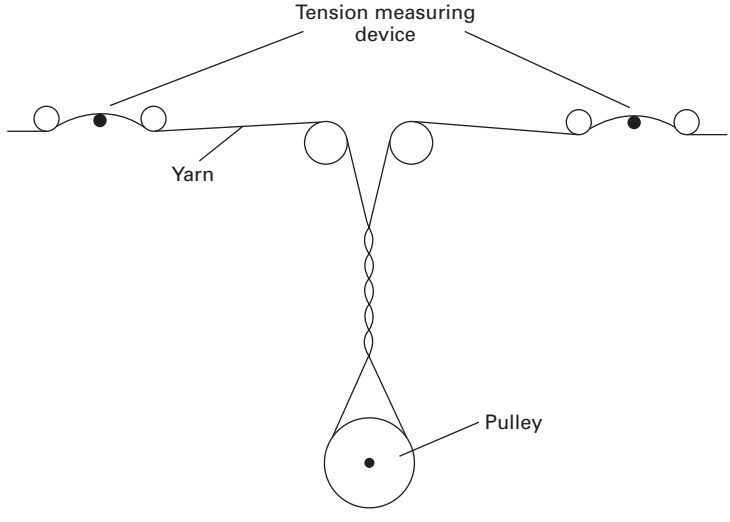

25.8 Measurement of yarn-on-yarn friction on a running yarn.

A very simple means of measuring friction is the inclined plane method [21]. Several turns of yarn are wound as a bow over a bridge and rested on a horizontal plate of the other material. This plate is gradually inclined. The coefficient of friction is equal to the tangent of the angle of inclination at which slippage starts. Howell and

Mazur [22] have used a similar method for studying the friction between single fibres. A lightly loaded loop of fibre is allowed to rest on another stretched fibre, which is mounted in a frame. The frame is initially horizontal and is then rotated until the loop of fibre just begins to slide down.

25.3 Empirical results

25.3.1 Friction, load and area of contact

The ratio of frictional force F to normal load N for fibres is found to decrease as the load is increased. In other words, Amontons' law is not obeyed. Some typical examples are given in Fig. 25.9. Among the various mathematical relations that have been used to fit the experimental data are the following:

$$F = \mu_0 N + \alpha S \tag{25.4}$$

$$\frac{F}{N} = A - B \log N \tag{25.5}$$

$$F = aN + bN^c \tag{25.6}$$

where S = area of contact, and μ_0, α, A, B, a, b and c are constants. The most successful relation has, however, been:

$$F = aN^n \tag{25.7}$$

where a and n are constants. This is a form of equation previously found by Bowden and Young [23] to apply to some non-metals: it was first applied to fibres by Lincoln [24] and by Howell and Mazur [22]. The value of the index n generally lies between 2/3 and 1, some typical values being given in Table 25.2.

If this relation holds, we can work out the effect of the areas of surfaces in

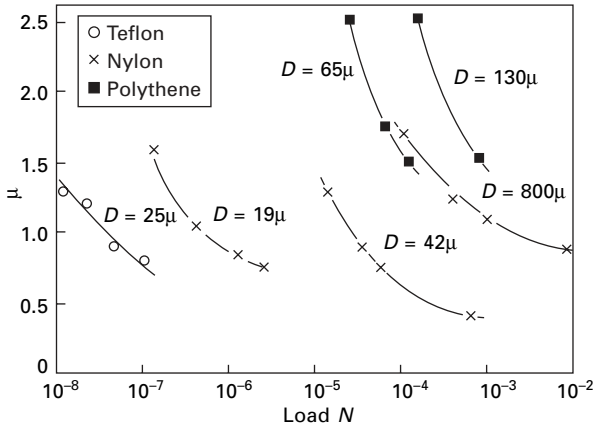

25.9 Variation of coefficient of friction of fibres with load (D = fibre diameter) [8].

Table 25.2 Values of *n*

(a) Results by Mazur [25] for single fibres crossed at right angles (fibre in vertical column sliding on fibre in horizontal column)

	Acetate	Nylon	Viscose rayon	*Terylene* polyester fibre	Wool*
Acetate	0.94	0.89	0.90	0.86	0.92
Nylon	0.86	0.81			
Viscose rayon	0.89	0.88	0.91	0.88	0.87
Polyester fibre *Terylene*	0.88				
Wool*	0.88	0.86	0.92	0.86	0.90

*Mean values, 'with' and 'against' scales.

(b) Other results

	n
Nylon monofil pulled over glass cylinder [26]	0.91
Acetate yarn pulled over chromium-plated cylinder [27]	0.8
Wool pulled over serge cylinder [28, 29]	0.75
Viscose rayon fibres crossed at right angles [30]	
static friction – normal finish	0.80–1.02†
– extracted	0.75–0.98
kinetic friction – normal finish	0.77–0.94
– extracted	0.64–0.99

† Value varying with filament linear density.

contact[2]. For a load N on an area A_1, the frictional force is $F_1 = aN^n$. For the same load on an area A_2, equal to xA_1, we may consider the total frictional force F_2 to be made up of the sum of the individual frictional forces f on x portions, each of area A_1, under loads N/x. But, from equation (25.7), it follows that:

$$f = a(N/X)^n \tag{25.8}$$

Therefore:

$$F_2 = \sum f = xa(N/x)^n \tag{25.9}$$

$$\frac{F_2}{F_1} = \frac{xa(N/x)^n}{aN^n} = x^{(1-n)} = \left(\frac{A_2}{A_1}\right)^{(1-n)} \tag{25.10}$$

The two classical laws of friction are thus replaced by the relations: $F = aN^n$, for constant apparent surface area in contact and $F = bA^{(1-n)}$, for constant load, where a

[2]The more detailed understanding of the nature of frictional force (discussed in Section 25.4.2) shows that the real determining factor is the number of points of true contact between the surfaces. For extensive apparent areas of contact, this number will be proportional to the overall geometric area of contact. This will not hold, however, for crossed fibres making a single-point contact, or for parallel fibres making contact along a line. It also follows that the friction is influenced by the roughness of the surface.

and b are constants, dependent on the area and load, respectively. It should be noted that a and b are not dimensionless and will thus vary with the units used. The parameter n should be a fundamental property of the materials, independent of geometry, although Guthrie and Oliver [30] have found an indication that it increases with filament linear density in staple-fibre rayon. The classical laws of friction will occur as the special case: $n = 1$.

Viswanathan [31] found experimentally that the parameter a is correlated with n to a fairly high degree over a wide range of fibres, and even better within a given fibre type. The values of a decrease approximately linearly from about 3 for $n = 0.6$ to 0.5 at $n = 0.9$. However, it must be remembered that a has the dimensions of $(\text{force})^{(1-n)}$, so that the results would look different in other units. There are theories that suggest reasons, and even equations, for the correlation.

Howell [29] has shown that, if equation (25.7) holds, then equation (25.2), relating the tensions in a yarn or fibre passing round a guide, is modified and becomes:

$$T_2^{(1-n)} = T_1^{(1-n)} + (1 - n)a\theta r^{(1-n)} \tag{25.11}$$

where r is the radius of the cylinder. In the limit, as n approaches 1, this equation reduces to:

$$T_2 = T_1 \, e^{a\theta(r/T_1)^{(1-n)}} \tag{25.12}$$

This form obviously reduces to the classical form when $n = 1$. Figure 25.10 shows a check of equation (25.11) for varying initial tensions and cylinder radii.

25.3.2 Static and kinetic friction: speed of sliding

The kinetic friction μ_k is usually less than the static friction μ_s. Some typical examples are given in Table 25.3. The difference affects the feel of the material. If it is large, the material is 'scroopy', that is, it will have a coarse, crunchy feel and will give a

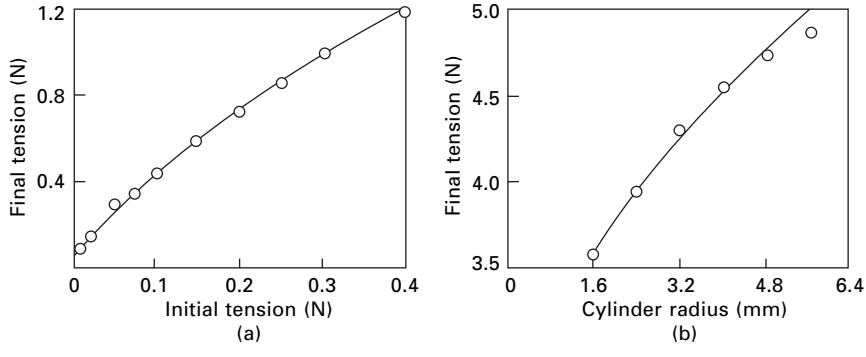

25.10 Check of equation (25.11) for (a) varying initial tension and (b) varying cylinder radius. The lines are the theoretical curves, and the points are experimental values for acetate yarn. For curve (a), $n = 0.8$, $a = 1.18$; for curve (b) $n = 0.8$, $a = 1.15$ [27].

Table 25.3 Static and kinetic friction [32]

	Static μ_s	Kinetic μ_k
Rayon on rayon	0.35	0.26
Nylon on nylon	0.47	0.40
Wool on wool		
with scales	0.13	0.11
against scales	0.61	0.38
fibres in same direction	0.21	0.15
Wool on rayon		
with scales	0.11	0.09
against scales	0.39	0.35
Wool on nylon		
with scales	0.26	0.21
against scales	0.43	0.35
Rayon on rayon [30]	0.22	0.14

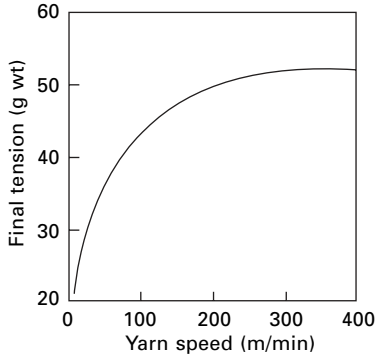

25.11 Variation of final tension after acetate yarn has passed over a guide at varying speeds [27] (50 g wt = 0.49 N).

fabric that rustles like silk, owing to the marked 'stick–slip' motion. This tendency will be reduced by any finish or lubricant that reduces the differences between μ_s and μ_k. The handle will then be softer.

At low speeds, going from 2 to 90 cm/min, Röder [33] noted a decrease in the friction, but at much higher speeds other workers have found that the friction increases as the speed increases. A typical result is shown in Fig. 25.11. It therefore seems likely that the frictional force passes through a minimum at around 1 m/min, due to mechanisms shown later in Fig. 25.25. The variation of friction with speed will have a considerable influence on the behaviour of fibres in drafting.

Cotton is exceptional in that even at low speeds the coefficient of friction increases with the speed of sliding. For example, Merkel [34] found that the coefficient of friction of single cotton fibres against cotton-covered cylinders increased steadily

with speed. Under medium-load conditions, the coefficient of friction was 0.23 at 3.6 cm/min, but it increased to 0.25 at 200 cm/min and to 0.39 at 4500 cm/min. One consequence of this is that the slippage of cotton, for example, in the deformation of needled fabrics, occurs more smoothly without the stick–slip effect characteristic of other fibres.

25.3.3 The state of the surface

The frictional force is changed if the surface is lubricated, either naturally, e.g. by waxes in cotton, or artificially, or by contamination with dirt or impurities. Figure 25.12 shows that, for acetate yarn with more than 1% of oil applied, the frictional force increases both as the oil content is increased and as the viscosity of the oil increases. However, fibres from which all traces of lubricant have been removed show high values of friction; thus, in one experiment [2], raw cotton on steel gave $\mu = 0.25$, whereas scoured cotton on steel gave $\mu = 0.7$, and lubricated scoured cotton on steel gave values of μ ranging from 0.14 to 0.35.

Bradbury and Reicher [35] have found that extremely high values of friction are obtained between flat continuous-filament yarns and glass if excessive precautions are taken to ensure the cleanliness of both surfaces. With nylon, the value of μ was at least 8, and a 50 gram weight could be supported on a short length of yarn looped over a glass rod, as shown in Fig. 25.13. This high value of friction was not found if the yarns were twisted, or if the glass surface was roughened by grinding: this suggests that the effect is associated with a high true area of contact (see Section 25.4.2). A similar effect was observed by King [36], who found a reduction in the friction of wool fibres on various materials when the surface was roughened. Values obtained are given in Table 25.4. The dependence on the physical state of the surface is also shown by the results in Table 25.5 for moulded and machined nylon. The newly moulded surface shows the highest coefficient of friction. Taylor and Pollet [38] have investigated the low force friction of several fabrics against engineering surfaces.

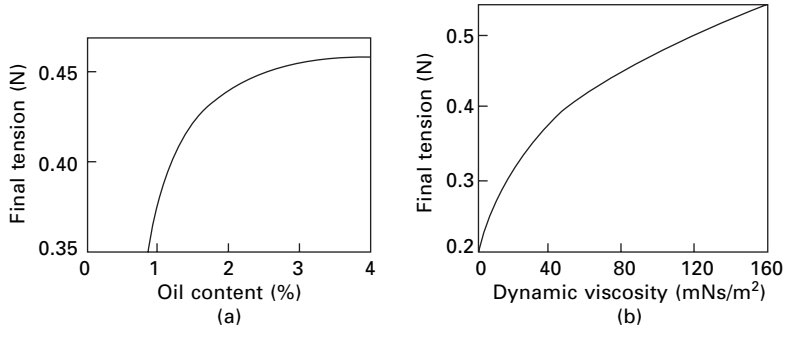

25.12 Variation of final tension after passage of acetate yarn over guide, for (a) varying amounts of oil on yarn and (b) varying viscosity of oil [25].

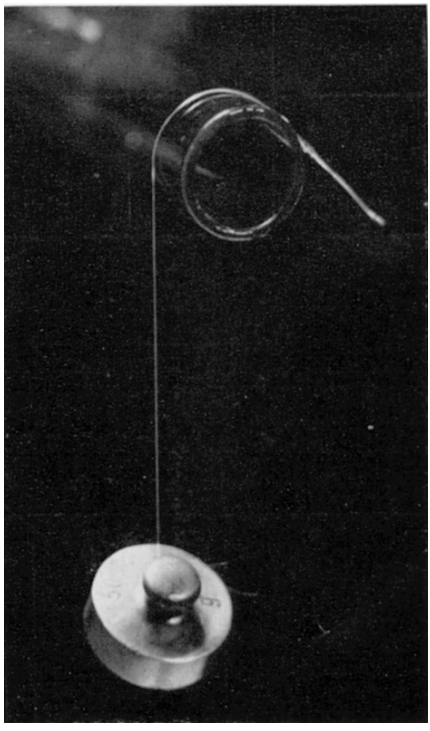

25.13 Demonstration of very high friction with clean nylon and glass [35].

Table 25.4 Effect of surface roughness: Values of μ for wool rubbed on various materials [36]

Material	Polished surface		Rough surface	
	With scales	Against scales	With scales	Against scales
Casein	0.58	0.59	0.47	0.57
Ebonite	0.60	0.62	0.50	0.61
Sheep's horn	0.62	0.63	0.52	0.63
Cow's horn	0.49	0.54	0.42	0.53

Table 25.5 Values of μ for moulded nylon [37]

	As received	Aged 30 min at 170 °C	Aged 5 months at 20 °C
Cold-moulded	0.70	0.45	0.55
Hot-moulded	0.65	0.45	0.55
Machined	0.45	0.40	0.45

25.3.4 Effect of water

The frictional force usually increases as the regain of the fibres is raised. Typical results are given in Fig. 25.14. Moghazy and Gupta [16] found that friction was higher in wet polypropylene and acrylic yarns than in dry ones.

25.3.5 Typical values of $\mu = F/N$

Although fibres do not have a true, constant coefficient of friction, it is useful to quote values of $\mu = F/N$ to express the magnitude of the friction under particular conditions. However, because this value of μ varies with so many of the experimental conditions (load, speed, area and geometry of contact, humidity, etc.) and because it is so dependent on the exact state of the surface, only typical values found in particular experiments can be quoted. Some examples are given in Table 25.6. They cannot be expected to have validity in other circumstances.

In general, values of μ for fibres and plastics range between 0.1 and 0.8, although, under extremely clean conditions, as described in Section 25.3.3, much higher values of fibre friction are found. Another exception is PTFE (known as *Teflon* in fibre form), which has an extremely low coefficient of friction, often less than 0.05, except at the very low loads shown in Fig. 25.9.

Table 25.7 gives values of coefficient of friction of yarns used in high-performance ropes [40]. High-modulus polyethylene (HMPE) fibres have an inherently low coefficient of friction, but the others will have special marine finishes, which reduce inter-fibre abrasion.

Behary *et al.* [41] studied the tribology of sized glass fibres and found wide variations in friction. One fibre had a unimodal distribution for μ ranging from 0.1 to 10 with scattered values up to 15, a peak at 3.5, a mean of 5 and a standard deviation

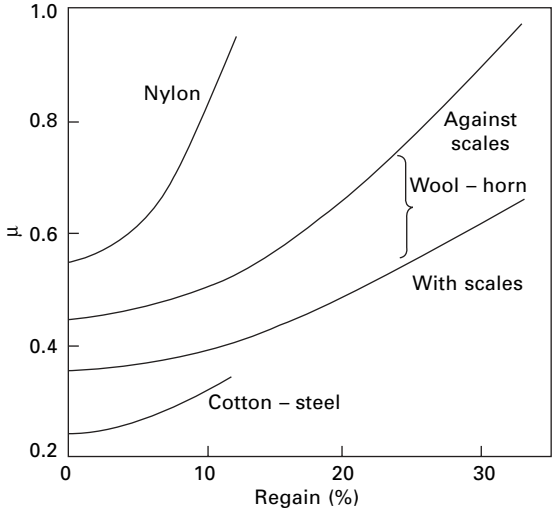

25.14 Change of coefficient of friction with regain for nylon on nylon, wool on horn [36] and cotton on steel [39].

Table 25.6 Typical values of μ (a) between fibres; (b) for yarns passing over guides [10]

(a)

	Crossed fibres [6]	Parallel fibres [32]
Nylon	0.14–0.6	0.47
Silk	0.26	0.52
Viscose rayon	0.19	0.43
Acetate	0.29	0.56
Cotton	0.29, 0.57	0.22
Glass	0.13	–
Jute	–	0.46
Casein	–	0.46
Saran	–	0.55
Terylene polyester fibre	–	0.58
Wool, with scales	0.20–0.25	0.11
Wool, against scale	0.38–0.49	0.14

(b)

	Hard steel	Porcelain	Fibre pulley	Ceramic
Viscose rayon	0.39	0.43	0.36	0.30
Acetate, bright	0.38	0.38	0.19	0.20
Acetate, dull	0.30	0.29	0.20	0.22
Grey cotton	0.29	0.32	0.23	0.24
Nylon	0.32	0.43	0.20	0.19
Linen	0.27	0.29	0.19	–

Table 25.7 Yarn-on-yarn friction results. From Noble Denton and National Engineering Laboratory (40]

	Load range (g)	Coefficient of friction μ		
		Mean sliding	Mean static	Maximum
Aramid				
Kevlar 29 (961)	100–1600		0.157	0.167
Kevlar 29 (960)	100–1500		0.137	0.150
Twaron 1000	100–1200		0.165	0.180
Twaron 1020	100–2500		0.131	0.138
Technora	100–2200	0.117		
LCP				
Vectran	100–2700		0.144	0.151
HMPE				
Spectra 1000	200–4500	0.058		0063
Dyneema SK60	2000–6000	0.061		0.064
Polyester				
Diolen 855TN	100–1500		0.092	0.099
Trevira 785	100–2500		0.060	0.064
Seagard IW81	100–1900		0.02	0.096

of 1.7. Another fibre with a different finish had a biomodal distribution with peaks at 1.25 and 6.25 and values from 0.25 to 9. They used atomic force microscopy to observe the fibre surfaces and related the frictional behaviour to the nature of the contacts between fibres. In another paper [42], they report on stick–slip behaviour.

Moghazy and Gupta [16] found that triangular and trilobal polypropylene monofilament shad lower friction that circular monofilaments.

25.3.6 Surface damage on rubbed fibres

The nature of the damage to the surface of fibres when they are subject to friction is of intrinsic interest and also leads to an understanding of the nature of the frictional force. Figure 25.15 shows a nylon filament that has been rubbed with a platinum

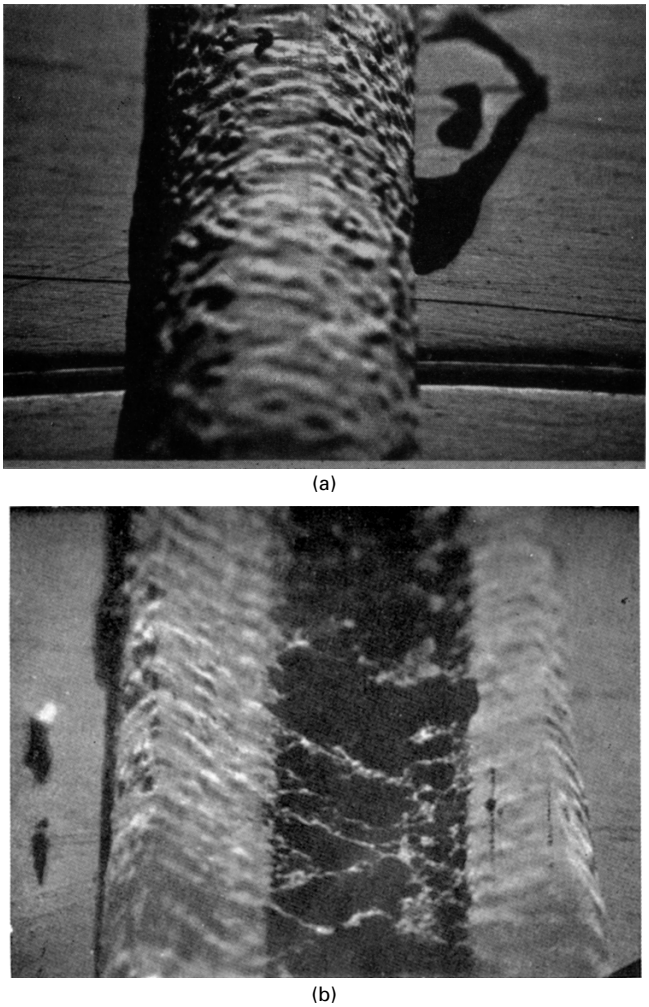

25.15 Effect of friction by platinum slider on nylon monofilament [43]: (a) low load, 0.39 N; (b) high load, 2.8 N.

slider under various loads, viewed by reflection electron microscopy. At low loads, there is a narrow track in which the fibre is slightly flattened, but at higher loads there is a marked deformation, and severe tearing of the surface occurs at the centre of the track. The concave shape of the track is probably due to reduced elastic recovery in the centre, where the deformation is greatest. Other examples of surface damage are shown in the electron micrographs of the surface of acetate fibres that have passed over guides (Fig. 25.16).

There is other evidence that material may be plucked out of the fibre surface during rubbing. Figure 25.17 shows particles of acetate (after dyeing) that were left on a glass rod rubbed with an acetate fibre, under the excessively clean conditions

25.16 Acetate fibre abraded by passing over a ceramic guide at 300 m/min. Damage is due to fibre sticking to a guide and then breaking away [4].

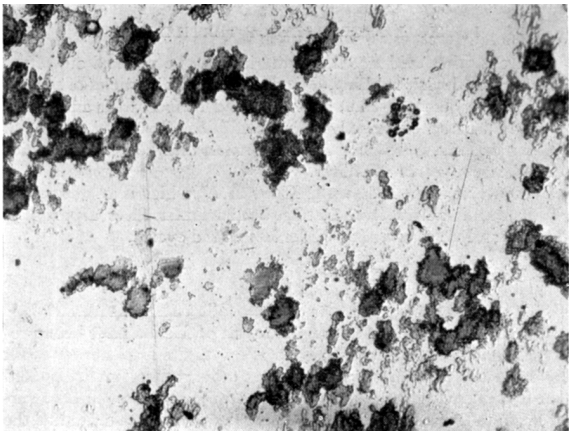

25.17 Particles of acetate left on glass rod, after rubbing with acetate fibre [35].

described in Section 25.3.3. Similar deposits were observed with nylon and polyester fibres, but not with viscose rayon or silk fibres. The reverse effect is shown in Fig. 25.18, which is an autoradiograph of radioactive silver that has been transferred to a PVC surface after a silver slider has passed over it.

25.4 The nature of friction

25.4.1 General theory

Over the centuries, many explanations of friction have been proposed. Amontons suggested that it was due to the force needed to lift one surface over the irregularities in the other; others have suggested that it is due to attractive forces between the atoms on the two surfaces, or to electrostatic forces. These theories all assume that the surfaces remain separate and, although they may sometimes play some part, the work of Bowden and Tabor [5, 44] showed that the predominant effects are usually an actual union, or welding, of the two surfaces at points of real contact, and the breaking of these junctions when sliding starts.

The surfaces of most materials are irregular if studied on a small enough scale: only in exceptional cases (for example, the cleavage planes of a crystal of mica) will they be smooth on the molecular scale. Bringing two surfaces into contact is therefore

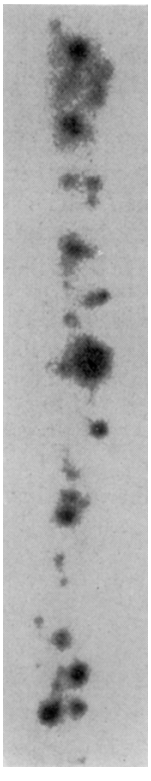

25.18 Radioactive silver left on polyvinyl chloride surface after rubbing [43].

like 'turning Switzerland upside down and putting it on top of Austria. Contact only occurs at the tips of the peaks' [44]. If a load is applied, the pressure at the few points of real contact is very great, and they squash down until the area in contact is adequate to support the load.

The nature and extent of the deformation will depend on the mechanical properties of the materials. Metals flow plastically under high loads, and the flow will continue until the pressure at the points of contact is reduced to the yield pressure, when it will support the load without further deformation. The condition for equilibrium is shown graphically in Fig. 25.19. If A is the total area of real contact, we have:

$$p_y = N/A \tag{25.13}$$

$$A = N/p_y \tag{25.14}$$

where N = applied load and p_y = yield pressure.

Thus the area of real contact is proportional to the applied load. Under the intense pressure, and an accompanying temperature rise, the junctions weld together, as illustrated in Fig. 25.20. In order to allow sliding, these junctions must be broken by shearing. The resistance to this, which is the frictional force F, will be given by:

$$F = SA \tag{25.15}$$

where S = shear strength of the weaker material. But, on substituting from equation (25.13), this gives:

$$F = \frac{S}{p_y} N = \mu N \tag{25.16}$$

Since S and p_y are both constants, being mechanical properties of the materials, this is Amontons' law with $\mu = S/p_y$. As the relation between load and contact area is linear, the total area in real contact will be independent of the number of points of contact. This explains the classical law that friction is independent of the overall area

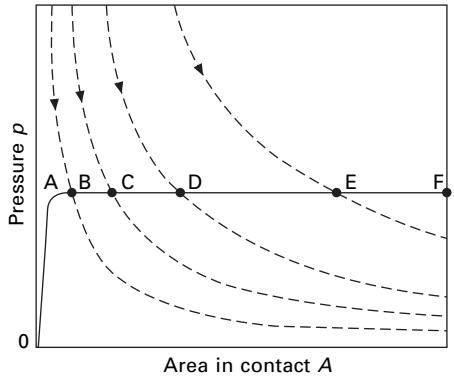

25.19 Deformation of metal contacts. The full line represents the load-deformation curve of the metal, with a elastic region, OA, and a region of plastic flow, AF. The dotted lines are pressure–area curves for constant loads. Equilibrium occurs at the intersections, B, C, D, E, of the full and dotted lines.

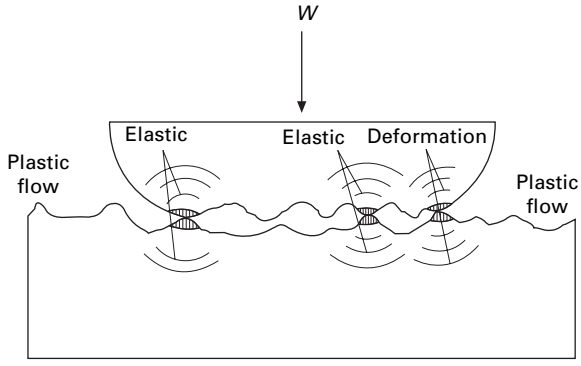

25.20 Deformation at points of real contact, showing welded junctions. After Bowden and Tabor [44].

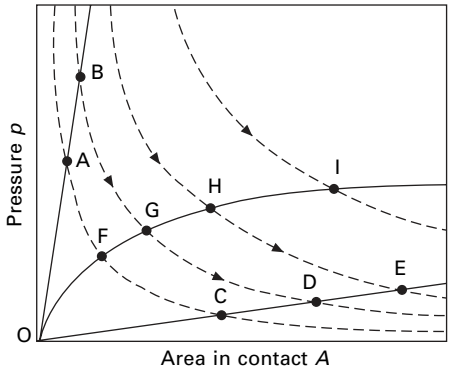

25.21 Deformation of elastic and viscoelastic materials. OB is the line for a hard elastic material, such as diamond; OE is the line for a soft elastic material, rubber; and OI is the curve for a viscoelastic material. Equilibrium occurs at the points of intersection with the pressure–area curves (dotted).

of contact. Bowden and his colleagues have produced a great deal of evidence in support of this theory in its application to metals: the values of μ agree with the above expression; the damage to the surface, the portions of metal plucked up, the metal transferred from one surface to the other, the evidence of strains below the surface, and the form of the track left after sliding show that welding and shearing must have occurred. They have found that, if one surface is much harder than the other, an additional force is needed to plough out a track in the soft metal for the asperities on the hard surface. This force will also contribute to the friction.

They have applied similar theories to non-metals. For brittle solids, such as rock salt, Amontons' law is obeyed, and the behaviour is similar to that in metals, but, in solids that are either very hard, such as diamond, or have a very large elastic deformation, such as rubber, the behaviour is different. With these materials, the deformation within the elastic range is sufficient to give support to the load. This is illustrated in Fig. 25.21. In neither case is the yield pressure reached. The relation between load

and area of real contact under conditions of elastic deformation depends on the geometry of the contacts and has been studied by Hertz [45].

For spheres in contact, $A \propto N^{2/3}$. Since we should still have $F = SA$, this would give $F \propto N^{2/3}$, a result that agrees with experimental results for diamond and rubber. This condition would be expected to apply approximately to the contact between asperities on an extended surface. However, the number of points of contact will affect the proportion of the load borne by each contact, and, since the relation between load and area is non-linear, this will affect the total area of contact. Thus the magnitude of the frictional force will depend on the roughness of the surface and on the overall area of contact.

For two cylinders at right angles, the Hertz formulae give $A \propto N^{2/3}$, and for two cylinders in contact along a line they give $A \propto N^{1/2}$.

25.4.2 Application to fibres

The damage to the surfaces of fibres and plastics during sliding shows that there has been a marked deformation of the surface and welding together at points of contact. The essential mechanism of friction is thus the same as that for the other materials discussed in the last section. The friction will depend on the force needed to shear the junctions, and, in general, calculations of shear strength of plastics from friction measurements, by means of equation (25.15), have shown reasonable agreement with bulk measurements of shear strength.

Experimentally, the frictional force is given by $F \propto N^n$, where the index n is less than 1 but is usually greater than that to be expected from a purely elastic deformation. The index will depend on the viscoelastic properties of the material, which determine the shape of the curve relating deformation to pressure. Figure 25.21 includes an example of a curve, not unlike typical fibre stress–strain curves, that would give values intermediate between the elastic deformation, also shown in Fig. 25.21, and the plastic flow of Fig. 25.19.

The relations will also depend on the geometry of the system. Pascoe and Tabor [8] have investigated the effect of the diameter of crossed fibres that make contact at a single point and deform as shown in Fig. 25.22. Working on a large scale with

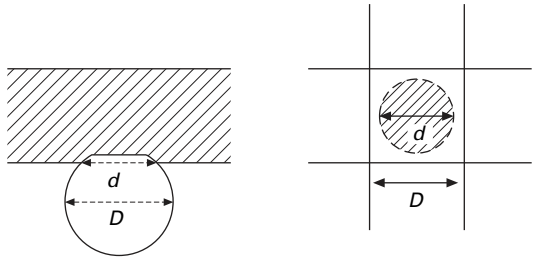

25.22 Deformation of crossed fibres under load.

Perspex cylinders 1 cm in diameter, they found that the diameter d of the circle of contact fitted the following relation over a wide load range:

$$N \propto d^{2.7} \tag{25.17}$$

Similar results were obtained with steel spheres pressed on various polymers.

The only parameter defining the shape of the deformation is the ratio d/D, where D is the diameter of the cylinder. This parameter will determine the distribution of strains, and hence of stresses, in the cylinders. Consequently, the mean pressure must be a function of d/D, that is:

$$\frac{N}{\pi d^2/4} = f\left(\frac{d}{D}\right) \tag{25.18}$$

If the function is assumed to be a power function, we can put:

$$\frac{N}{d^2} = K\left(\frac{d}{D}\right)^x \tag{25.19}$$

$$N = K\frac{d^{2+x}}{D^x} \tag{25.20}$$

Comparison with the experimental results given by the relation (25.17) shows that $x = 0.7$, so that we have:

$$ND^{0.7} = Kd^{2.7} \tag{25.21}$$

This equation fits the experimental results on cylinders of different diameters.

The frictional force is given by:

$$F = S\,A = S\,(\pi d^2/4) \tag{25.22}$$

But from the general relation, equation (25.20), we see that:

$$d^2 = \left(\frac{N\,D^x}{K}\right)^{2/(2+x)} \tag{25.23}$$

Therefore, in general:

$$F = kN^{2/(2+x)}D^{2x/(2+x)} \tag{25.24}$$

In the special case, with $x = 0\ 7$, this gives:

$$F = kN^{0.74}\,D^{0.52} \tag{25.25}$$

$$\mu = \frac{F}{N} = kN^{-0.26}\,D^{0.52} \tag{25.26}$$

Figure 25.23 shows that this relation fits the experimental results for nylon.

The dependence of friction on the force needed to shear the material in the region of welded junctions does not apply when the strength of the weld is itself very low. This happens with the inert material PTFE, which shows very poor adhesion to other

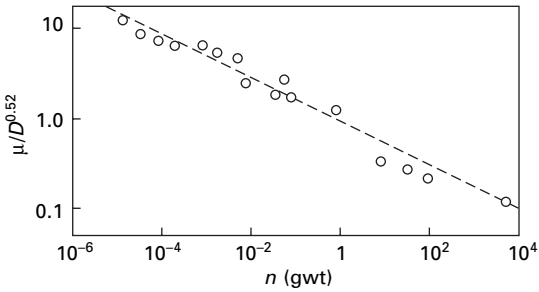

25.23 Check of equation (25.25) for nylon in the form of fibre, bristles and spheres [8], $\mu/D^{0.52}$ being plotted against N on logarithmic coordinates. The straight line has a slope of –0.26 (1 g wt = 9.81 m N).

surfaces, and is the cause of its low coefficient of friction.

Gupta and Moghazy [46] have made a detailed study of the interaction of asperities on fibre surfaces. They derive the following expression for the empirical equation (25.7) with specific shear strength appearing as in equation (25.16):

$$F = S\,[C_M\,K^{-n}\,m^{1-n}]\,N^n \tag{25.27}$$

where C_M depends on the distribution of normal load in the contact area, K is related to the hardness of the areas in contact, given by the relation between pressure P and area A, $P = K\,A^{(1-n)/n}$ and m = number of asperities in contact. The index n depends on the deformation behaviour of the material as discussed above. This model has been applied to the frictional behaviour of polypropylene, acrylic and cotton fibres [16, 20].

25.4.3 Lubricated conditions

Compared with its effect on metals, where it may reduce the value of μ from 1 to 0.05, lubrication has comparatively little effect on the friction of fibres and will not usually reduce the value of μ below about 0.2. The behaviour is usually thought of as boundary lubrication in which the layer of lubricant is not sufficiently thick to mask the asperities on the surface. Under these conditions, a good lubricant acts by forming monolayers on the surface and preventing the adhesion of the two surfaces at points of contact. There are then very few contacts between the materials, and most of the friction results from the force needed to shear the lubricant film itself.

If greater quantities of lubricant are present, then we may have conditions of hydrodynamic lubrication, in which there is a comparatively thick film of fluid between the surfaces and the friction results from the viscous resistance to flow. In conventional bearing lubrication under hydrodynamic conditions, the coefficient of friction is found to be a single-valued function of ZN/P, where Z is the viscosity of the oil, N is the angular velocity of the journal and P is the nominal pressure on the bearing. The analogous quantity for a yarn passing over a guide is ZV/W, where V is the yarn velocity and W is the load on the guide. Hansen and Tabor [47] have analysed Lyne's data [27], and more of their own, and found, as shown in Fig. 25.24,

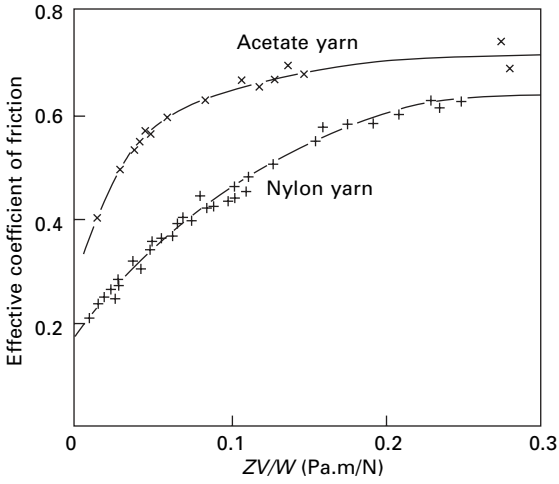

25.24 Effective coefficient of friction plotted against *ZV/W* for acetate yarn and nylon yarn on steel, lubricated with white mineral oils. The point cover variations in speed, pin radius, pre-tension and oil viscosity.

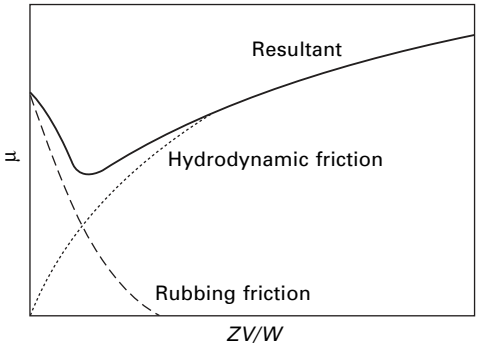

25.25 Combination of rubbing friction and hydrodynamic friction.

that the coefficient of friction is a single-valued function of *ZV/W*. They conclude that, for moderately high values of *ZV/W* (high speed, low loads), hydrodynamic lubrication is the dominant factor.

At low speeds (or high loads), an oil film would not be maintained between the surfaces, and rubbing friction would be dominant. This decreases with increased speed. Consequently, a combination of rubbing friction at low speeds and hydrodynamic friction at high speeds would give a minimum in the friction, as is shown in Fig. 25.25. This is in agreement with the experimental results.

25.5 The friction of wool

25.5.1 Experimental

The friction of the wool fibre depends on the direction in which it is pulled: the

resistance is greater when it is pulled against the scales than when it is pulled with them. This is known as the *directional frictional effect* (DFE), and the various combinations that can occur are illustrated in Fig. 25.26. This effect has important technical consequences, since it means that, in a mass of wool, individual fibres will show preferential movement in one direction and will continually entangle themselves with the remaining fibres: this is the process of felting.

Some experimental values for the directional frictional effects of wool are given in Table 25.8. It has been shown that the effect persists, though to a reduced extent, when the fibres are lubricated or coated with thin films of gold or silver [48]. In

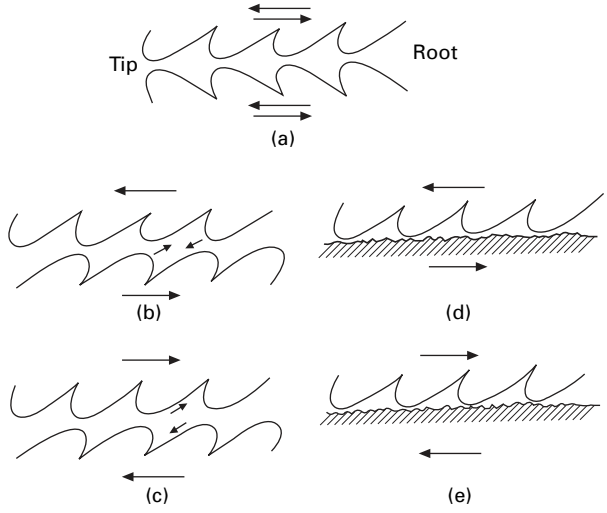

25.26 Directional friction in wool: (a) between fibres placed in same direction; (b) between fibres against scales; (c) between fibres with scales; (d) on plane surface, against scales; (e) on plane surface, with scales.

Table 25.8 Directional friction in wool

	Value of μ	
	With scales	Against scales
Dry wool (twisted fibres) 13	0.11	0.14
Wool in water (twisted fibres) 13	0.15	0.32
Wool unswollen on ebonite swollen in benzene [36]	0.58	0.79
Wool swollen in water on ebonite unswollen [36]	0.62	0.72
Wool swollen in water on ebonite swollen in benzene [36]	0.65	0.88
Wool on horn, dry [41]	0.3	0.5
Wool on horn, wet pH 4.0 [49]		
untreated	0.3	0.6
chlorine-treated	0.1	0.1
alcoholic-caustic-potash-treated	0.4	0.6
sulphuryl-chloride-treated	0.6	0.7

Other values are included in Tables 25.3, 25.4 and 25.6.

water, or other swelling agents, the difference in the coefficients of friction is greater than it is in air. On the other hand, the difference is less after mechanical abrasion or chemical treatments, designed to reduce shrinkage, which attack the outer layer of the wool fibre.

25.5.2 Theory of the directional frictional effect

The occurrence of directional friction has almost invariably been ascribed to the geometric form of the scales. Other explanations, such as Martin's view [50] that there was an asymmetrical molecular field at the surface of the fibre, appear far-fetched and are not supported by the experimental evidence. The various theories have been reviewed by Makinson [51].

The simplest geometrical theory is that the wool fibre acts as a ratchet, with the scales interlocking with one another or catching against asperities on another surface. Motion against the scales would be strongly resisted, since it would involve rupture or deformation of the scales. Makinson [51] regards this as an effective explanation, and indicates that a ploughing mechanism would also be effective. Lincoln [52] has given a more sophisticated geometrical theory, which applies the general idea that friction is due to the shearing of real areas of contact.

Figure 25.27 shows the contact between an idealised wool scale structure and asperities on another surface. The scale surfaces are assumed to be inclined at an angle α, so that a tangent through the point of contact between an asperity and the scale surface makes an angle α with a line parallel to the axis of the wool fibre. Contact may also occur between an asperity and the scale edge, with the tangent at the contact making an angle β with the fibre axis. For slippage to occur, there must be shearing parallel to the tangents at each point of contact. We must therefore consider the relations between the forces when contact occurs at an angle, as shown in Fig. 25.28.

The resultant force R acting at the contact may be resolved either into components W and F acting perpendicular and parallel to the direction of motion, or into components N and P acting perpendicular and parallel to the tangent at the contact. If the angle between these directions is θ, we must have:

$$N = W \cos \theta + F \sin \theta \tag{25.28}$$

$$P = F \cos \theta - W \sin \theta \tag{25.29}$$

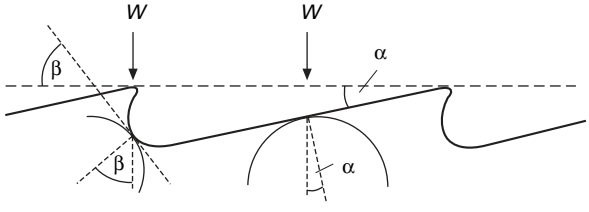

25.27 Contact between scale structure and asperities on a surface.

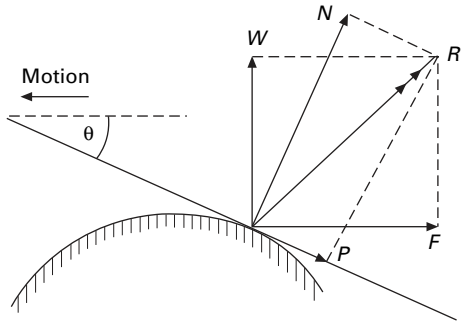

25.28 Geometry of contact.

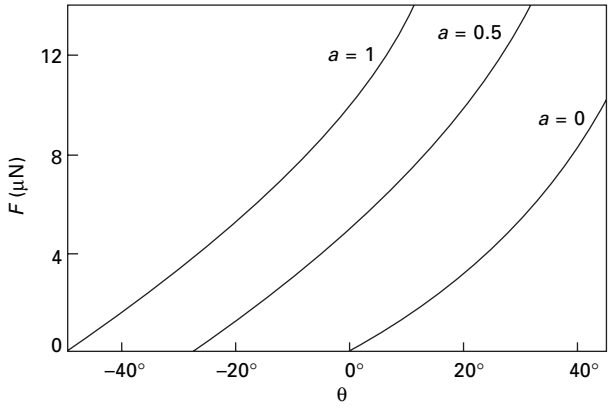

25.29 Variation of F with θ, with n = 2/3 (after Lincoln [52]).

For slippage to occur, the junction must be sheared. The force necessary to do this will be given by the general frictional relation $P = aN^n$.

Substituting from equations (25.28 and 25.29), we have

$$F \cos \theta - W \sin \theta = a(W \cos \theta + F \sin \theta)^n \tag{25.30}$$

Lincoln gives a graphical solution of this equation, showing values of F for various values of a and θ, when n = 2/3. This value of n is applicable to elastic deformation at the junction. Figure 25.29 is taken from this graph and shows the variation of F with θ. The resistance to motion decreases as the value of θ decreases. When θ is positive, there will be resistance to motion even if $a = 0$, that is, if the friction is zero. It should be noted that negative values of θ correspond to motion in the reverse direction to that shown in Fig. 25.28.

We can now consider the application of this result to the contact between two surfaces. If the asperities on the surfaces are completely random, then large and small, positive and negative, values of θ will be equally likely for motion in any direction and there will be no directional effect.

In wool, however, there is a regular arrangement of asperities, the scale structure. Figure 25.27 shows that, for motion against the scales, the two types of contact will

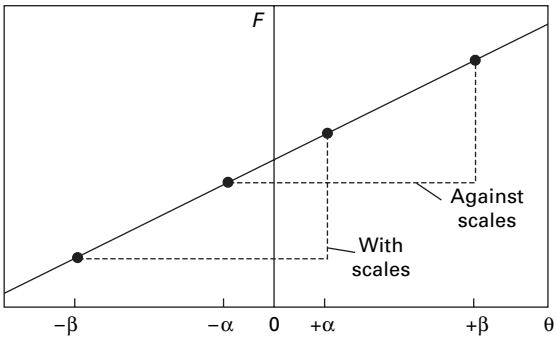

25.30 Combination of values of α and β, for motion with and against scales.

have values of θ equal to +β and –α, whereas for motion with the scales the values will be –β and +α. From the combination of these values, shown in Fig. 25.30, it would appear obvious that the frictional force would be greater against the scales.

There are, however, complications, which have the effect that the frictional force is not a simple mean of the two values of *F*. Firstly, there are more α contacts than β contacts, since there is a greater length of scale surface than of scale edge. Secondly, the geometry of the contacts will be different and will influence the value of α and the distribution of the load. Thirdly, the values of α depend on the range of values of the scale angle, and the values of β may range up to π/2, depending on the position of the contact round the scale edge, though the effective negative values of β will be limited by the condition: $F \geq 0$. These factors will reduce the difference in the friction by causing the net force to be nearer that given by the β contacts than that given by the α contacts. In principle, it may even cause a reversal of the directional effect, but the detailed analysis given by Lincoln, considering the three-dimensional view of fibre contacts, shows that this would not happen.

25.6 References

1. W. L. Balls. *Studies of Quality in Cotton*, Macmillan, London, 1928, p. 80.
2. E. Moss. *Brit. J. Appl. Phys.*, 1951, **2**, Suppl. No. 1, 19.
3. F. P. Bowden and L. Leben. *Proc. Roy. Soc.*, 1939, **A169**, 371.
4. V. Peck and W. Kaye. *Text. Res. J.*, 1954, **24**, 295.
5. F. P. Bowden and D. Tabor. *The Friction and Lubrication of Solids*, Oxford University Press, London, 1950; revised reprint, 1954.
6. J. C. Guthrie and P. H. Oliver. *J. Text. Inst.*, 1952, **43**, T579.
7. E. H. Mercer and K. R. Makinson. *J. Text. Inst.*, 1947, **38**, T227.
8. M. W. Pascoe and D. Tabor. *Proc. Roy. Soc.*, 1956, **A235**, 210.
9. G. M. Abbott and P. Grosberg. *Text. Res. J.*, 1966, **36**, 928.
10. H. Buckle and J. Pollitt. *J. Text. Inst.*, 1948, **39**, T199.
11. J. H. Jung, T. J. Kang and J. R. Youn. *Textile Res. J.*, 2004, **74**, 1085.
12. P. Grosberg and D. E. A. Plate. *J. Text. Inst.*, 1971, **62**, 116.
13. J. Lindberg and N. Gralén. *Text. Res. J.*, 1948, **18**, 287.
14. B. S. Gupta, K. W. Wolf and R. W. Postlethwint. *Surg. Gync. Obst.*, 1985, **161**, 12.
15. N. Fair and B. S. Gupta. *J. Soc. Cosmetic Chem.*, 1982, **33**, 229.

16. Y. E. El Moghazy and B. S. Gupta. *Textile Res. J.*, 1993, **63**, 219.
17. D. S. Taylor. *J. Text. Inst.*, 1955, **46**, P59.
18. E. Lord. *J. Text. Inst.*, 1955, **46**, P41.
19. J. W. S. Hearle and A. K. M. M. Husain. *J. Text. Inst.*, 1971, **62**, 83.
20. Y. E. El Moghazy and R. M. Broughton. *Textile Res. J.*, 1993, **63**, 465.
21. J. B. Speakman and E. Stott. *J. Text. Inst.*, 1931, **22**, T339.
22. H. G. Howell and J. Mazur. *J. Text. Inst.*, 1953, **44**, T59.
23. F. P. Bowden and J. E. Young. *Proc. Roy. Soc.*, 1951, **A208**, 444.
24. B. Lincoln. *Brit. J. Appl. Phys.*, 1952, **3**, 260.
25. J. Mazur. *J. Text. Inst.*, 1955, **46**, T712.
26. H. G. Howell. *J. Text. Inst.*, 1954, **45**, T575.
27. D. G. Lyne. *J. Text. Inst.*, 1955, **46**, P112.
28. A. J. P. Martin and R. Mittelmann. *J. Text. Inst.*, 1946, **37**, T269.
29. H. G. Howell. *J. Text. Inst.*, 1953, **44**, T359.
30. J. C. Guthrie and P. H. Oliver. *J. Text. Inst.*, 1952, **43**, T579.
31. A. Viswanathan. *J. Text. Inst.*, 1966, **57**, T30.
32. B. Olofsson and N. Gralén. *Text. Res. J.*, 1950, **20**, 467.
33. H. L. Röder. *J. Text. Inst.*, 1955, **46**, P84.
34. R. S. Merkel. *Text. Res. J.*, 1963, **33**, 84.
35. E. Bradbury and A. Reicher. *J. Text. Inst.*, 1952, **43**, T350.
36. G. King. *J. Text. Inst.*, 1950, **41**, T135.
37. D. Summers-Smith. *Research*, 1955, **8**, S17.
38. P. M. Taylor and D. M. Pollet. *J. Textile Inst.*, 2000, **91**, Part 1, 1.
39. J. A. Morrow. *J. Text. Inst.*, 1931, **22**, T425.
40. Noble Denton and National Engineering Laboratory. Fibre Tethers 2000, Final Report, Noble Denton, London, quoted in H. A. McKenna, J. W. S. Hearle and N. O'Hear, *Handbook of Fibre Rope Technology*, Woodhead Publishing, Cambridge, UK, 2004, p. 70.
41. N. Behary, C. Caze, A. Perwuelz and A. El Achari. *Textile Res. J.*, 2000, **70**, 700.
42. N. Behary, C. Caze, A. Perwuelz and A. El Achari. *Textile Res. J.*, 2001, **71**, 187.
43. J. A. Chapman, M. W. Pascoe and D. Tabor. *J. Text. Inst.*, 1955, **46**, P3.
44. F. P. Bowden and D. Tabor. *Friction and Lubrication*, Methuen, London, 1956.
45. H. Hertz. *J. Reine Angew. Math.*, 1881, **92**, 156.
46. B. S. Gupta and Y. E. El Moghazy. *Textile Res. J.*, 1991, **61**, 547.
47. W. W. Hansen and D. Tabor. *Text. Res. J.*, 1957, **27**, 300.
48. H. M. S. Thompson and J. B. Speakman. *Nature*, 1946, **157**, 804.
49. E. H. Mercer. *Nature*, 1945, **155**, 573.
50. A. J. P. Martin. *J. Soc. Dyers Col.*, 1944, **60**, 325.
51. K. R. Makinson. *Wool Sci. Rev.*, 1972, No. **42**, 2.
52. B. Lincoln. *J. Text. Inst.*, 1954, **45**, T92.